Platinum Nanoparticle Interaction with Chemically Modified Highly Oriented Pyrolytic Graphite Surfaces

De-Quan Yang and Edward Sacher*

Regroupement Québécois de Matériaux de Pointe, Département de Génie Physique, École Polytechnique, C.P. 6079, succursale Centre-Ville, Montréal, Québec H3C 3A7, Canada

Received November 7, 2005. Revised Manuscript Received February 2, 2006

Ar, N_2, O_2, and H_2O radio frequency (13.56 MHz) plasma treatments have been carried out on insulator-supported samples of highly oriented pyrolytic graphite (HOPG). The HOPG surface was found to be minimally damaged by all the plasma treatments, which break C−C bonds and form free radicals in the outermost few layers. These free radicals subsequently react, on exposure to air, forming various oxidation products; both XPS and photoacoustic FTIR indicate that these include C−OH, C═O, and −COOH. Pt was deposited onto these samples by evaporation, forming nanoparticles. After plasma treatment, the dimensions of the Pt nanoparticles were ∼3.5−4 nm, compared to ∼6 nm on untreated HOPG, and they no longer diffused laterally; this indicates enhanced interfacial adhesion for all these plasma treatments. The occurrence of oxidation products strongly suggests that the increased Pt nanoparticle adhesion to the treated HOPG surface is due to their presence.

Introduction

Highly oriented pyrolytic graphite (HOPG) is a two-dimensional solid with strong covalent bonding within each layer and only weak van der Waals interactions between neighboring layers. It is widely used as a substrate for nanoparticle deposition,[1,2] due to its atomic flatness, ease of cleavage, relative inertness in air, and weak interaction with deposited nanoparticles. Due to this weak interaction, the nanoparticles are able to diffuse across the HOPG surface and coalescence on contact. Correspondingly, scanning probe microscopic characterizations of nanoparticles on these surfaces are limited because of tip-induced particle displacement.

HOPG is the preferred surface for oxidation and gas−solid surface reaction studies,[3−25] since it offers a comprehensible structure and chemical stability not offered by other forms of carbon, such as graphite fibers and carbon composites;[4,5,12] oxidation-induced defects may act as nucleation centers to obtain a homogeneous distribution of nanoparticles.[7] It was previously noted[26] that the plasma surface modification of Dow Cyclotene, a low permittivity polymer, can greatly enhance nanoparticle adhesion due to the formation of functional chemical groups and free radicals on the treated surface.

Several studies[7−9,18] have shown that nanometer- to micrometer-sized surface defect pits may form on the HOPG surface; the pit size, its number density, and its shape are dependent on the plasma gas mixture, temperature, pressure, and treatment time. These pits may be used as "molecule corrals" for the study of the ordering of self-assembled molecular monolayers[17] or as templates for the formation of metal and semiconductor nanostructures.[4,7,27−35] As previ-

* Corresponding author. Tel: (514) 340-4711, ext 4858. Fax: (514) 340-3218. E-mail: edward.sacher@polymtl.ca.

(1) Henry, C. R. *Surf. Sci. Rep*. **1998**, *31*, 231.
(2) Brune, H. *Surf. Sci. Rep*. **1998**, *31*, 125.
(3) Yang, R. T.; Wong, C. *J. Chem. Phys.* **1981**, *75*, 4471.
(4) Wong, C.; Yang, R. T.; Halpern, B. L. *J. Chem. Phys.* **1982**, *78*, 3325.
(5) Nowakowski, M. J.; Vohs, J. M.; Bonnell, D. A. *Surf. Sci. Lett*. **1992**, *271*, L351.
(6) Nowakowski, M. J.; Vohs, J. M.; Bonnell, D. A. *J. Am. Ceram. Soc*. **1993**, *76*, 279.
(7) Chang, H.; Bard, A. J. *J. Am. Chem. Soc*. **1991**, *113*, 5588.
(8) Chu, X.; Schmidt, L. D. *Carbon* **1991**, *29*, 1251.
(9) Chu, X.; Schmidt, L. D. *Surf. Sci.* **1992**, *268*, 325.
(10) You, H. X.; Brown, N. M. D.; Alassadi, K. F. *Surf. Sci.* **1993**, *284*, 263.
(11) Fournier, J.; Miousse, D.; Brossard, L.; Menard, H. *Mater. Chem. Phys.* **1995**, *42*, 181.
(12) O'Kell, S.; Pringle, S.; Jones, C. *J. Adhes.* **1996**, *56*, 261; Serp, P.; Corrias, M.; Kalck, P. *Appl. Catal. A: Gen.* **2003**, *253*, 337.
(13) Bourelle, E.; Konno, H.; Inagaki, M. *Carbon* **1999**, *37*, 2041.
(14) Paredes, J. I.; Martínez-Alonso, A.; Tascón, J. M. D. *Chem. Commun.* **2002**, 1790; *J. Mater. Chem*. **2000**, *10*, 1585.
(15) Paredes, J. I.; Martínez-Alonso, A.; Tascón, J. M. D. *Langmuir* **2003**, *19*, 7665.
(16) Lu, X. K.; Huang, H.; Nemchuk, N.; Ruoff, R. S. *Appl. Phys. Lett*. **1999**, *75*, 193.
(17) Patrick, D. L.; Cee, V. J.; Beebe, T. P., Jr. *Science* **1994**, *265*, 231.
(18) Tracz, A.; Kalachev, A. A.; Wegner, G.; Rabe, J. P. *Langmuir* **1995**, *11*, 2840.
(19) Hahn, J. R.; Kang, H. *J. Vac. Sci. Technol. A* **1999**, *17*, 1606.
(20) Hahn, J. R.; Kang, H. *Phys. Rev. B* **1999**, *60*, 6007.
(21) Kinoshita, H.; Umeno, M.; Tagawa, M.; Ohmae, N. *Surf. Sci.* **1999**, *440*, 49.
(22) Ruffieux, P.; Groning, O.; Schwaller, P.; Schlapbach, L.; Groning, P. *Phys. Rev. Lett*. **2000**, *84*, 4910.
(23) Rousseau, B.; Estrade-Szwarckopf, H.; Thomann, A. L.; Brault, P. *Appl. Phys. A.* **2003**, *77*, 591.
(24) Estrade-Szwarckopf, H. *Carbon* **2004**, *42*, 1713.
(25) Portail, M.; Faure, J. B.; Angot, T.; Layet, J. M. *Surf. Sci.* **2005**, *581*, 24.
(26) Yang, D.-Q.; Sacher, E. *J. Phys.: Condens. Matt*. **2002**, *14*, 7097; Yang, D.-Q.; Martinu, L.; Sacher, E.; Sadough-Vanini, A. *Appl. Surf. Sci.* **2001**, *177*, 85.
(27) Ahn, Y.-O.; Seidl, M. *J. Appl. Phys*. **1995**, *77*, 5558.
(28) Hövel, H.; Becker, T.; Bettac, A.; Reihl, B.; Tschudy, M.; Williams, E. J. *J. Appl. Phys*. **1997**, *81*, 154.
(29) Stable, A.; Eichhorst-Gerner, K.; Rabe, J. P.; González-Elipe, A. R. *Langmuir* **1998**, *14*, 7324.
(30) Houbertz, R.; Weber, U.; Hartmann, U. *Appl. Phys. A.* **1998**, *66*, S149.
(31) Carroll, S. J.; Palmer, R. E.; Mulheran, P. A.; Hobday, S.; Smith, R. *Appl. Phys. A.* **1998**, *67*, 613.

10.1021/cm052453e CCC: $33.50
Published on Web 03/09/2006

ously indicated,[34−36] surface defects, such as these pits, and free radical sites (in the absence of oxidation) severely limit the diffusion of metallic atoms and nanoparticles on the HOPG surface by enhancing their interfacial adhesion.

Both scanning tunneling (STM) and atomic force (AFM) microscopies, due to their high resolution capabilities, have been extensively used to study the oxidation kinetics of the HOPG surface[4−7,13−15,17−19] and, as a result, these processes are reasonably well understood from the morphological point of view. However, because HOPG strongly absorbs in the IR region, less chemical information has been obtained by this method than by X-ray photoelectron spectroscopy (XPS). The C1s and O1s XPS spectra of the treated HOPG surface are found to become more complex[24] during oxidation, while the compound C1s spectral line shapes[34] are affected by the presence of defects,[35] as well as oxidation products. Due to the structural similarity of HOPG and carbon fibers, which are widely used in heterogeneous catalysis as substrates for nanoparticle deposition, HOPG presents itself as an ideal model for fundamental studies of such catalysis, which uses catalyst nanoparticles of a uniform size and a high number density.

While weak catalyst−substrate interaction gives a large particle size distribution and a lower particle number density, surface modifications offer a method for decreasing both particle size and distribution and increasing number density: [37−39] extensive studies[38−42] have indicated that the oxidation of carbon-containing materials accomplishes this. Generally speaking,[38,39] the dispersion of precious metal catalysts on carbon-containing materials increases with oxidation, although the interaction between many metals and functionalized surfaces has not yet been studied and understood.

Here, we explore the surface functionalization of HOPG, using several low-energy plasma environments. These treatments all result in chemical groups being introduced at the outer layers of the surface, with less damage than found with other treatments. Both XPS and photoacoustic FTIR are used to identify surface functional groups and their effect on deposited Pt nanoparticles.

Experimental Section

Grade ZYA HOPG was obtained from Advanced Ceramics, Inc. It was cleaved with adhesive tape just prior to plasma treatment and then inserted into the X-ray photoelectron spectrometer or into a high vacuum evaporator for Pt deposition. Pt deposition was performed, at a pressure of 10^{-8} Torr, by electron beam heating; 5 nm of Pt was deposited at a deposition rate of 0.01 nm/s.

(32) McBride, J. D.; Van Tassell, B.; Jachmann, R. C.; Beebe, T. P., Jr. *J. Phys. Chem. B.* **2001**, *105*, 3972.
(33) Zhu, Y.-J.; Schnieders, A.; Alexander, J. D.; Beebe, T. P., Jr. *Langmuir* **2002**, *18*, 5728.
(34) Yang, D.-Q.; Sacher, E. *Surf. Sci.* **2002**, *504*, 125.
(35) Yang, D.-Q.; Sacher, E. *Surf. Sci.* **2002**, *516*, 43.
(36) Yang, D.-Q.; Sacher, E. *J. Appl. Phys.* **2001**, *90*, 4768.
(37) Rodriguez-Reinoso, F. *Carbon* **1998**, *36*, 159.
(38) Fraga, M. A.; Jordao, E.; Freitas, M. M. A.; Faria, J. L.; Figueiredo, J. L. *J. Catal.* **2002**, *209*, 355.
(39) Rodríguez-Reinoso, F. *Carbon* **1998**, *36*, 159.
(40) Coloma, F.; Sepulveda-Escribano, A.; Fierro, J. L. G.; Rodriguez-Reinoso, F. *Langmuir* **1994**, *10*, 750.
(41) Boehm, H. P. *Carbon* **1994**, *32*, 759.
(42) Auer, E.; Freund, A.; Pietsch, J.; Tacke, T. *Appl. Catal. A.* **1998**, *173*, 259.

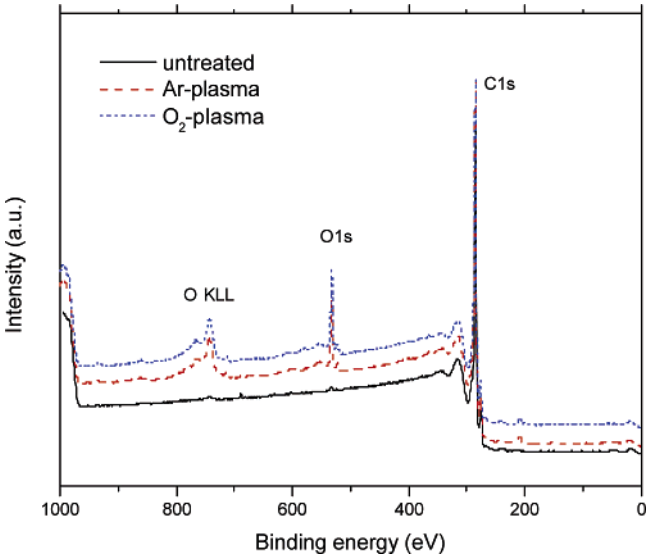

Figure 1. XPS survey scans of HOPG surfaces on various plasma treatments.

The surface modification of the HOPG samples was carried out in a capacitively coupled radio frequency (RF, 13.56 MHz) plasma discharge, using O_2, Ar, H_2O, or N_2 gases. The samples were mounted on a RF-powered electrode, 10 cm (4") in diameter. To minimize damage and to eliminate ion bombardment of the HOPG surface, the HOPG was electrically insulated from its electrode. The chamber was pumped to a base pressure below 10^{-5} Torr prior to introducing the high purity gas, and the following process parameters were used: gas flow, 20 sccm; working pressure, 200 mTorr; RF power, 100 W; treatment time, 2 min. A dc self-bias voltage of −200 V developed on the electrode when RF power was applied.

XPS analysis was carried out in a VG ESCALAB 3 Mark II, using nonmonochromated Mg Kα X-rays (1253.6 eV), at a base pressure of $<10^{-10}$ Torr. High-resolution spectra were obtained at a perpendicular takeoff angle, using a pass energy of 20 eV and 0.05 eV steps. The instrument resolution was ~0.7 eV. After Shirley background removal, the component peaks were separated by the VG Avantage V1.62 program (Thermo VG Scientific), using previously determined peak energies and widths. The peak energies were calibrated by placing the major C1s peak (C−C) at 284.6 eV.

Ex situ contact-mode atomic force microscopy (C-AFM) was carried out on a digital multimode scanning probe microscope. For these measurements, the integral gain was set at 2, the proportional gain was set at 3, and the deflection set point was set at 0 V. Commercially available silicon nitride cantilevers, with a spring constant of 0.5 N m^{-1}, a typical tip radius of 10−20 nm, and a tip half angle of 35°, were used. The tip-scanning rate was 2 Hz, and 512 lines were used per image.

PA-FTIR spectra were obtained using a He-purged MTEC 300 photoacoustic cell in a Bio-Rad FTS 6000 spectrometer. The 5 kHz modulation frequency that was used assured that the entire sample thickness was probed. The spectral resolution was set at 4 cm^{-1}.

Results

A. XPS of the Plasma-Treated HOPG Surface and of Deposited Pt. Typical XPS survey scans of the untreated HOPG surface, as well as after Ar and O_2 plasma treatments, are found in Figure 1. The untreated HOPG surface shows a small O1s signal, which increases in intensity on plasma treatment. High-resolution C1s spectra are shown in Figure

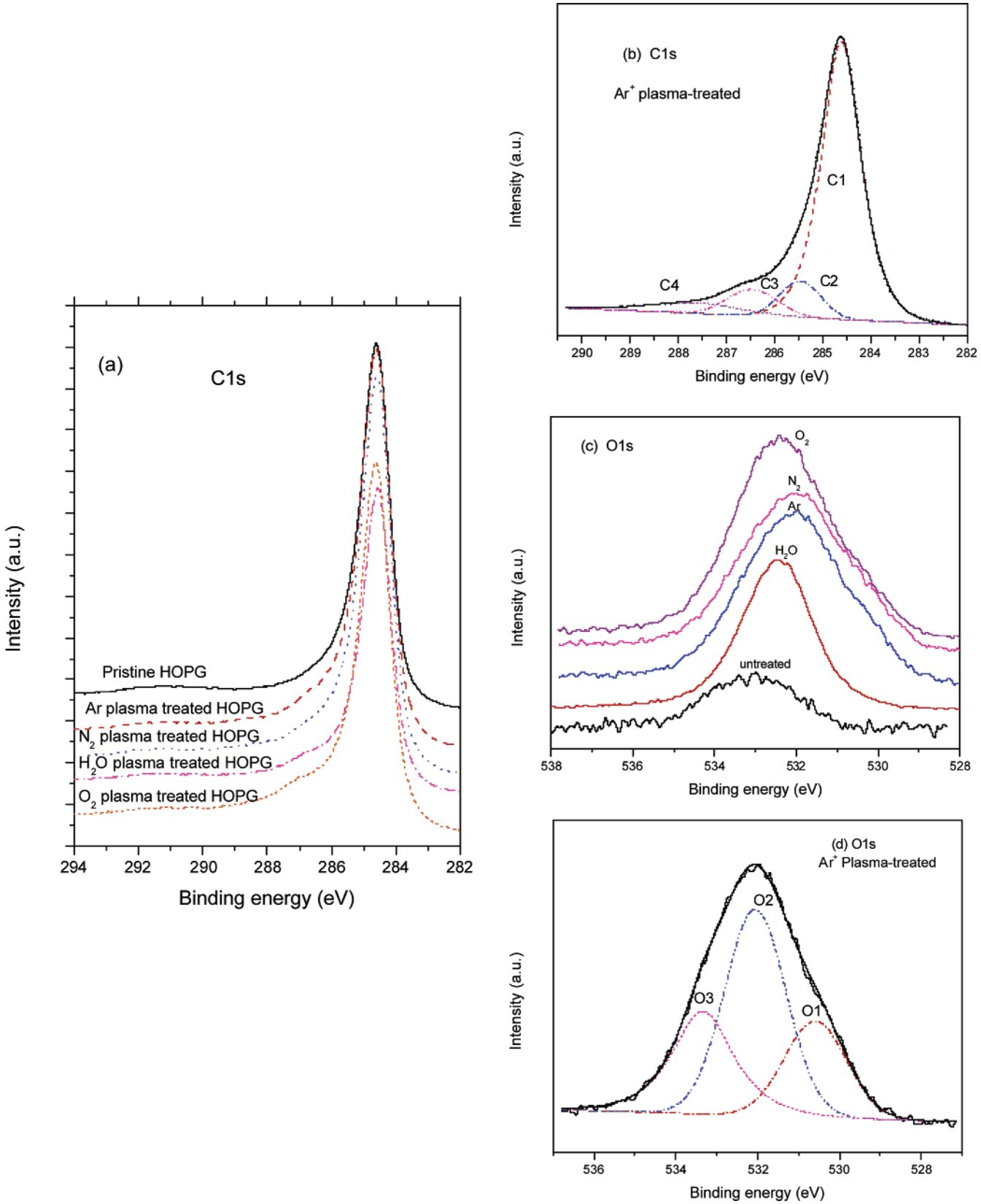

Figure 2. High-resolution XPS scans of (a) the HOPG C1s spectra after various surface treatments, (b) the HOPG C1s deconvolution after Ar treatment and air exposure, (c) the HOPG O1s spectra after various surface treatments, and (d) the HOPG O1s deconvolution after Ar treatment and air exposure.

2a, with component peaks for Ar treatment separated in Figure 2b. The component separation is based on the untreated HOPG results of our previous XPS studies,[33,34,35] where four components were found. These are C1 (284.6 eV, undamaged alternant hydrocarbon, with extensive electron delocalization), C2 (285.6 eV, defect alternant hydrocarbon, with limited electron delocalization), C3 (286.5 eV, sp^3 defect bonds), and C4 (287.8 eV, the C2 shake-up satellite; the C1 shake-up satellite is beyond the range of the scan). In the case of plasma treatment and subsequent

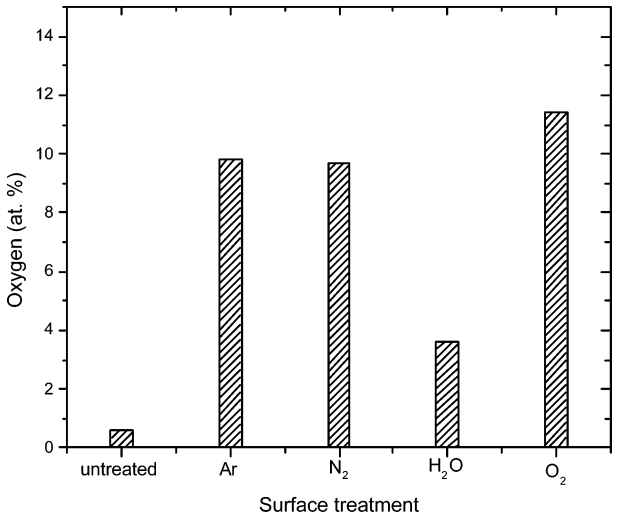

Figure 3. Atomic percent oxygen as a function of plasma treatment.

exposure to atmosphere, *additional* peaks, due to the introduction of oxidized species, superimpose on the original peaks, and must be taken into account. These include C−OH (∼286.5 eV), C═O (∼287.5 eV), and COOH (∼289 eV). Their presence is signaled by increases in the intensities of the already existing C2−C4 peaks rather than by the obvious addition of new peaks. The full width at half-maximum (fwhm) of peak C1 is unchanged on plasma treatment; because the fwhm is directly related to surface damage,[34,35] this indicates that minimum damage has occurred on our low-energy plasma treatments, less than reported by others,[12,23] but similar to what was found for hyperthermal atomic oxygen treatment.[21]

As the intensities of the oxidized C1s components increase, following plasma treatment, the O1s spectra in Figure 2c exhibit an increase in both intensity and in lower binding energy components. The peaks are separated in Figure 2d and are attributed[43−46] as follows: O1 (530.5 eV, an O-containing species with enhanced electron density at the emitting O, to be discussed later), O2 (532.6 eV, C═O/C−OH), and O3 (533.7 eV, COOH). Their atomic percentages are seen in Figure 3, where it is evident that all the plasma treatments have caused substantial increases on subsequent air exposure.

Both the oxygen content on the HOPG surface and the relative concentrations of the components are functions of the surface plasma environment, as seen in Figure 3 and Table 1, respectively. One notes (1) the lack of the O1 component for both untreated and H_2O plasma-treated HOPG and (2) the relatively lower oxygen and C−H contents on H_2O plasma treatment, compared to the other plasma treatments.

As noted earlier, the overlap of C1s components from two sources (i.e., defects and oxidation) makes it difficult to separate them. Further, the N1s spectra on N_2 plasma treatment (not shown) indicates a trace of nitrogen bonded to carbon, similar to what we found[47] for N implanted into HOPG by a 2 keV N_2^+ beam.

Table 1. Comparison of O1s Spectral Components for Various Plasma Treatments[a]

surface treatments	O1	O3	total % O
untreated HOPG	0	1.33	0.8
Ar	0.47	0.55	10
N_2	0.52	0.68	10
O_2	0.62	0.23	12
H_2O	0	0.42	4

[a] Normalized to O2 = 1.

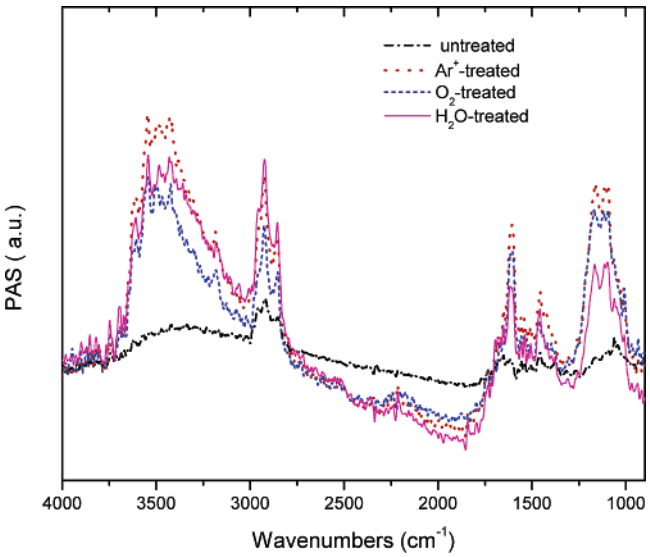

Figure 4. Photoacoustic FTIR of various plasma-treated HOPG surfaces.

Pt, vapor-deposited onto untreated HOPG, to be discussed in a subsequent paper, shows evidence of surface oxidation on exposure to atmosphere, similar to what we found for gold:[48] in particular, the Pt4f doublet peaks show evidence of small amounts of higher valent components, while the O1s peak shows a component at just under 531 eV (obviously different than the O1 component mentioned earlier), whose intensity increases several times on air exposure, indicative of surface oxidation. On exposure to atmospheric water vapor, Pt−OH groups are produced.

B. Photoacoustic FTIR of the Plasma-Treated HOPG Surface. Figure 4 shows PA-FTIR spectra of various plasma-treated HOPG surfaces. The broad, intense band at ∼3000−3500 cm^{-1} is due to O−H stretching, and that at ∼2800−2900 cm^{-1} is due to $-CH_n$ ($n = 1-3$) stretching. The strong peak at ∼1609 cm^{-1} is due to −C═C bending in the HOPG skeleton, while a shoulder at ∼1630−1750 cm^{-1} is attributed to −C═O stretching. The band at 1450 cm^{-1} is due to $-CH_n$ deformation, while the band at ∼1000−1250 cm^{-1} is due to −C−O− (i.e., hydroxyl, ether) stretching. To compare the spectra, we have normalized all peaks to −C═C−; their ratios are given in Table 2. Considering Tables 1 and 2, we find that the surface chemical groups present are similar for Ar, O_2, and N_2 plasma treatments, but there is less $-CH_n$ on O_2 plasma treatment. Further, for H_2O treatment, for

(43) Briggs, G.; Beamson, D. *Anal. Chem.* **1993**, *65*, 1517.
(44) Albers, P.; Karl, A.; Mathias, J.; Ross, D. K.; Parker, S. F. *Carbon* **2001**, *39*, 1663.
(45) Proctor, A.; Sherwood, P. M. A. *Carbon* **1983**, *21*, 53.
(46) Kozlowsky, C.; Sherwood, P. M. A. *J. Chem. Soc. Faraday Trans.* **1984**, *80*, 2099.
(47) Yang, D.-Q.; Sacher, E. *Surf. Sci.* **2003**, *531*, 185.
(48) Sylvestre, J.-P.; Poulin, S.; Kabashin, A. V.; Sacher, E.; Meunier, M.; Luong, J. H. T. *J. Phys. Chem. B* **2004**, *108*, 16864.

Table 2. Comparison of Major PA FTIR Peaks for Various Plasma Treatments[a]

bands	Ar^+	N_2	O_2	H_2O
ν_{OH} (3450 cm^{-1})	1.75	1.45	1.59	2.65
ν_{CH_n} (2920 cm^{-1})	1.36	1.54	1.22	2.70
δ_{CH_n} (1450 cm^{-1})	0.52	0.62	0.35	0.68
ν_{C-O-} (1150 cm^{-1})	1.30	1.56	1.37	1.30

[a] Normalized to $\nu_{C=C}$ skeletal stretching peak (1605 cm^{-1}) = 1.

which no O1 XPS component exists, there is significantly more of both −OH and $-CH_n$ than for other plasma treatments, suggesting that the H_2O plasma participates in the grafting of −OH and −H to the HOPG surface, rather than simply breaking bonds.

C. AFM of Pt Deposition on the Plasma-Treated HOPG Surface. There is only a slight increase in HOPG surface roughness after these plasma treatments, less than 0.2 nm over a 1 μm × 1 μm scan, with no dependence on plasma treatment; these images are not shown here. Figure 5a presents an AFM image of a nominal 5 nm of Pt deposited onto untreated HOPG surface and, for comparison, Figure 5b shows the same nominal 5 nm of Pt deposited onto an Ar plasma-treated surface; the results for other plasma-treated surfaces are comparable. Clearly, the Pt nanoparticles on untreated HOPG are significantly larger than on the plasma-treated surfaces. Those on the untreated surface also appear to be nonuniformly distributed, with a larger size distribution. Figure 6 shows the nanoparticle dimensions, including probe tip contributions; although the particle dimensions are smaller, this contribution is less.[49]

The nanoparticle size reduction on all plasma treatments indicates[34−36] enhanced interaction with the Pt nanoparticles. This was shown by contact mode AFM, using increased tip pressures: it was found possible to move the Pt nanoparticles on untreated HOPG, using a set point (uncalibrated tip pressure) of 2; however, after all plasma treatments, even two scans at a set point of 10 could not move the Pt nanoparticles. While the dimensional data suggest marginally stronger interaction on H_2O plasma treatment, this has not been confirmed because that slight enhancement has not yet proved measurable.

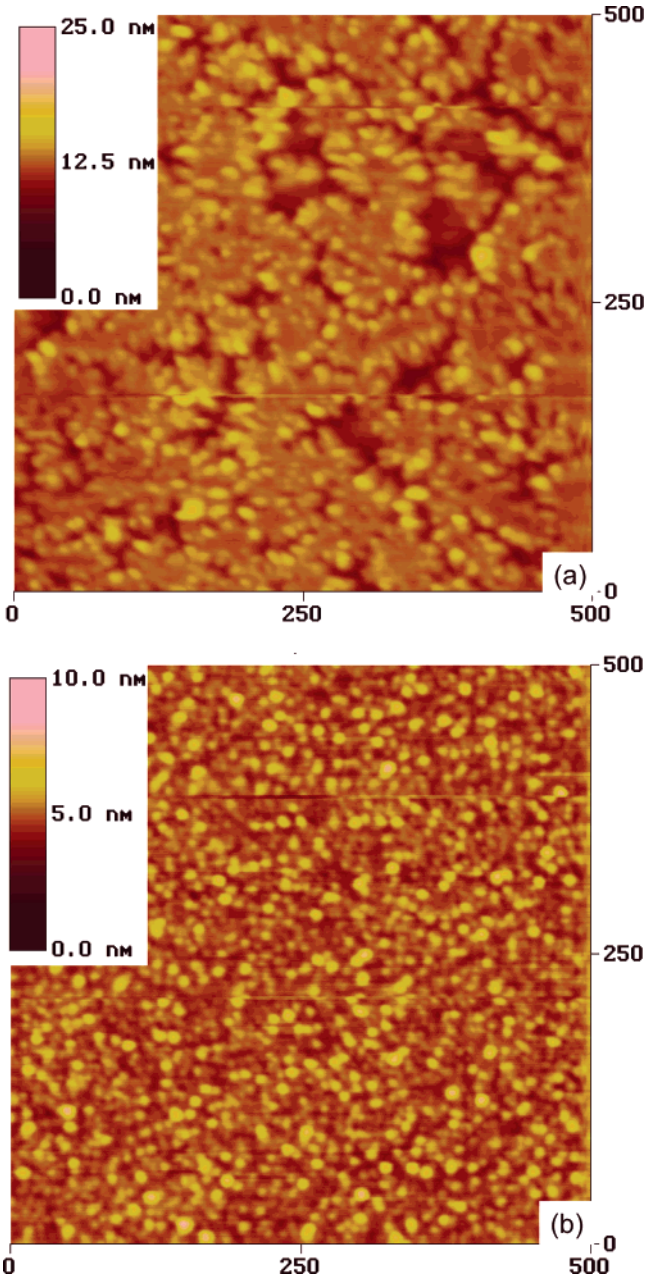

Figure 5. Comparison of contact AFM images of 5-nm-thick Pt evaporated onto HOPG surfaces: (a) untreated and (b) O_2 plasma-treated.

Discussion

Both XPS and photoacoustic FTIR indicate that the treatment of HOPG by several plasmas results in mild surface damage as a C−C bond in the outer layers undergoes chain scission to create two −C• free radicals; subsequent reaction with atmospheric water gives C−OH and C−H. The further reaction of the alcoholic C with OH, perhaps on further bond breaking, leads to a *gem*-diol, which is unstable and loses water to give HC═O; the final oxidation product of a primary C atom is COOH. Ether formation, in a free radical milieu, requires H abstraction from C−OH, by −C•, to give −C−O• and C−H, followed by reaction between −C−O• and −C•.

Despite the fact that all the plasma treatments give similar surface modifications, the H_2O plasma treatment is noticeably different: it produces a lower level of surface oxidation (Table 1), yet higher levels of both C−OH and $-CH_n$ (Table 2); in addition, the absence of an increase near 287.5 eV in the C1s XPS spectrum, on exposure to atmosphere, strongly suggests the absence of aldehyde or ketone, something that is difficult to confirm by IR because any C═O stretching peak would exist as a small shoulder, at ∼1660 cm^{-1}, where other peaks already exist (see Figure 4). This difference from other plasma treatments appears to be due to the presence of species, in a H_2O plasma, that not only cause bond scission but also react with the free radicals produced.[50] Thus, further reaction with atmosphere, on exiting the plasma chamber, is minimal.

(49) Yang, D.-Q.; Xiong, Y.-Q.; Guo, Y.; Lu, W.-G. *J. Mater. Sci.* **2001**, *36*, 263.

(50) Steen, M. L.; Hymas, L.; Havey, E. D.; Capps, N. E.; Kastner, D. G.; Fisher, E. R. *J. Membr. Sci.* **2001**, *188*, 97; Steen, M. L.; Jordan, A. J.; Fisher, E. R. *J. Membr. Sci.* **2002**, *204*, 34.

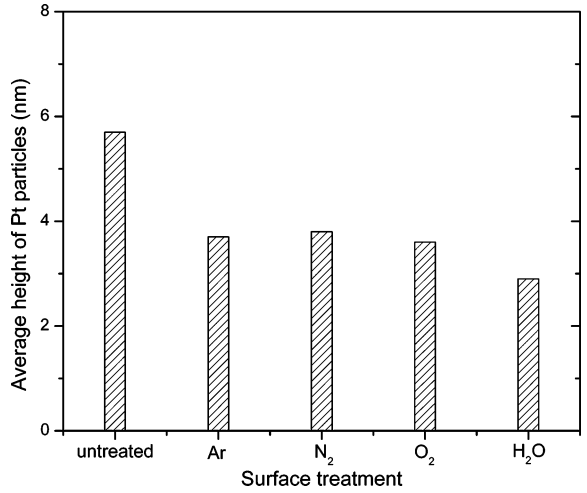

Figure 6. AFM images of average Pt nanoparticle heights as a function of plasma treatment.

Further, its O1s XPS spectrum contains no O1 component. This component clearly reflects the presence of a highly electronegative O-containing group. It is formed on Ar, O_2, and N_2 plasma treatments, but is present neither on untreated nor on H_2O plasma-treated HOPG. We tentatively attribute this to the presence of C−O• free radicals: the frontier orbital of a free radical is a singly occupied molecular orbital (SOMO), which, in the case of a C−O• free radical, lies closer to the lowest unoccupied molecular orbital (LUMO) of the HOPG onto which it is grafted than it does to the highest occupied molecular orbital (HOMO). SOMO−LUMO interactions[51] give rise to nucleophilic properties on the O•, especially when it is free to draw charge from the alternant hydrocarbon. Such free radicals do not exist on untreated HOPG, where the oxygen content is essentially undetectable, nor on H_2O plasma-treated HOPG, where the reactive species in the plasma react with them. The fact that they persist in Ar-, O_2-, and N_2-treated HOPG indicates that they cannot readily react with the O-containing species present in air, probably because they exist below the surface.

(51) Fleming, I. *Frontier Orbitals and Organic Chemical Reactions*; Wiley: New York, 1976; Chapter 5.

Previous STM/AFM studies[6,7,10,13−20,23] have indicated that both low-energy plasmas and ion bombardment result in the creation of point defects and etching (when fragmentation occurs). This produces vacancies, interstitials, nanoscale pits, and local disorder within a depth of one or two monolayers. These defects offer sites for Pt deposition, as was previously found by us for Cu deposition.[34,35] We also found, in those studies, that nanocluster surface diffusion is hindered by the presence of large amounts of defects, although strong interfacial adhesion was obtained only on the formation of chemical bonding across the nanoparticle-substrate interface. This necessitates surface functionalization. In the present case, this is accomplished by the formation of hydrogen bonds formed between the C−OH, C═O, and COOH at the HOPG surface and the Pt−OH at the nanoparticle surface, formed on atmospheric exposure. The additional influence of residual HOPG free radicals on the adhesion of Pt nanoparticles is presently being investigated.

Conclusions

We have found that Ar, O_2, N_2, and H_2O plasma treatments of the HOPG surface produce defects that react with plasma components, in the case of H_2O plasma treatment, or atmospheric components, in all other cases, to produce O-containing species (−C−OH, −C═O, −COOH) capable of hydrogen bonding. In a similar fashion, deposited Pt nanoparticles oxidize at their surfaces and react with the water vapor present, to form Pt−OH, capable of hydrogen bonding to the functionalized HOPG surface. This plays an important role in enhancing the adhesion of Pt to HOPG, as demonstrated by our contact AFM studies, which showed that strong contact forces were incapable of moving the Pt nanoparticles that were easily moved on the untreated HOPG surface.

Acknowledgment. The authors thank the Natural Sciences and Engineering Research Council of Canada and GM Canada for funding and Dr. Oleg Zabeida for help with the plasma treatments.

CM052453E